Field noise effects on NMR signals: Hahn echoes and CPMG.

by **Sykora** Stanislav
Extra Byte, Via Raffaello Sanzio 22C, Castano Primo, Italy 20022
published in **Stan's Library, Volume I**, May 2006 (www.ebyte.it/library/Library.html)

Abstract

Using techniques developed in an earlier article on field noise propagation into FID'a and 1D spectra, this study investigates the effects of various types of field fluctuations on Hahn echoes and CPMG echo trains.

Compared to an FID, the echoes (both single and multiple) refocus a substantial part of the induced phase errors, provided the field noise is Gaussian and its mean correlation time is not much smaller than τ (the time interval between the 90 and 180-degree pulses). For a normally distributed field noise, the echo-phase errors never exceed those of an FID at the same total time elapsed since the excitation pulse.

When the field is subject to a periodic or quasi-periodic modulation, there are τ values at which the re-focussing is very good, alternating with regions where the echo phase errors exceed those encountered in an FID. For a single echo the critical τ values center around odd multiples of T/2, T being the modulation period, while the 'good' ones are in the vicinity of integer multiples of T. This picture changes in a train of n echoes. Increasing n beyond 3, ever more *ample* regions of τ values with excellent field-error re-focussing alternate with ever narrower regions of severe *resonant error amplification*. The critical τ values are centered around odd multiples of T/4 and may all but preclude a successful application of a CPMG sequence. This, among other things, explains some the often observed striking - and so far only partially explained - CPMG artifacts.

The results provide a basis for the evaluation of errors due to field noise in those experimental techniques which use multiple spin echoes and/or spin-locking mechanisms. Due to field noise, averaged CPMG data are biased in a way which increases the apparent decay rate. Since this noise-induced decay factor is non-exponential, it can simulate/modify a non-exponential decay.

I. Introduction

Conceptually, this Note builds on a previous one (1), henceforth referred-to as **Part I**, which deals with the analysis of the effects of field noise/modulation on simple FID's and which the reader should consult also for basic assumptions and terminology.

The Hahn spin echo (2) is extensively used in a wide range of NMR applications such as, for example, T_2 measurements in LR-NMR and HR-NMR, refocusing pulses in HR-NMR, spin-diffusion measurements, sensitive plane selection and/or k-space navigation in MRI, flow imaging, receiver dead-time masking, etc. Be it protein structure determination, brain-cancer scan, NMRD profile of an elastomer, ex-situ measurement of a monument's masonry or a geo-prospecting well log, spin echoes are likely to be part of the procedure.

Understanding the statistical properties of echo fluctuations in an unstable main magnetic field is therefore of considerable importance across the whole of NMR.

This Note analyses the quantitative statistical relationship between spin echo phase instabilities and magnetic field fluctuations. Only the Hahn spin echoes induced by RF-pulses are considered, leaving for the moment out echoes induced by field-gradients which are used in many MRI techniques. Though gradient echoes sensitivity to field/gradient noise can certainly be investigated by methods similar to those adopted here, there are specifics which exceed the scope of this paper and will be investigated later. However, we will consider the generalization of the Hahn echo sequence consisting of trains of refocusing pulses, known as the Carr-Purcell-Meiboom-Gill (CPMG) sequence (3,4).

A well known, special phenomenon is the occasional exceptional sensitivity of CPMG spin echo trains to certain types of periodic magnetic field fluctuations. In his carrier as NMR service engineer, the Author has encountered practical cases when reliable CPMG measurements were all but precluded, for example, by field modulations due to i) stray fields from the electric wiring of a laboratory or ii) sample vibrations induced by a magnet cooling-water pump, floor vibrations induced by nearby heavy

machinery and even by loud music. Yet, quantitative studies of the phenomenon are extremely rare so that one usually concentrates on empirical detection and suppression of such field instabilities to a point where they no longer *appear* to have a significant effect on the echo train. This, of course, is understandable - except that one should be able to do so on the basis of a reliable theory permitting an objective assessment of the residual disturbances. Despite this necessity, the Author has found only one serious experimental NMR study carried out long time ago by Allerhand (5). Though some of the equations he deduced are still valid, they lack the generality required to cover all present-day applications and all types of field instabilities.

In order to maintain the theoretical treatment as self-coherent as possible, we will analyze the effect of field noise on a generic n-*th* echo in a CPMG echo train. This then includes the special case of n=1 corresponding to a single, isolated Hahn echo and even the case with n=0 (the zero-*th* echo) which, as we shall see, coincides formally with a plain FID and thus represents an independent check of the validity of the results.

Particular attention will be dedicated to sequences of n CPMG echoes *with equidistant timing*. Such trains of echoes, with n ranging sometimes into thousands, are used in both LR (low resolution) and HR (high resolution) NMR. In the LR version one often samples just one point of each echo (synchronized with the top of its amplitude) and acquires n such samples in each CPMG scan. The HR version is more time consuming since one needs to acquire a whole FID starting at the top the last (n-*th*) echo. Consequently, one can acquire in each scan just one echo which, however, contains the echoes of many individual spectral lines resolvable by standard Fourier Transform techniques. In both cases, it is the phase stability of the n-th echo which is to be determined.

Types of spin-echo instabilities

Consider the CPMG sequence $[(\pi/2)_x - \tau - (\pi)_y - \tau -$ acquisition$]$. The echo *amplitude* at time $t = 2\tau$ (the 'top' of the echo) contains a number of factors due to such diverse phenomena as transverse relaxation (T_2), self-diffusion (D), homonuclear couplings (J) and 'chemical' exchange, none of which affects its RF phase. On the other hand, spin echo eliminates (refocuses) the effects of field/RF offset[1], field inhomogeneity, chemical shifts and heteronuclear couplings.

Any spin-echo instability therefore arises from imperfections in one or more of the re-focussing phenomena. This leads to three broad classes of spin-echo fluctuations:

1) Instabilities due to **mean field/offset fluctuations** which have a *direct impact on the echo phase but not on its absolute magnitude*. When the echo signal is acquired using a phase- & offset-insensitive detection method (diode detection, RF envelope detection or signal power detection) such instabilities don't show up - a fact which can be used to discriminate them from the other types. Instabilities of this kind (see Part I for a more detailed discussion) are the most common ones in practice and the only ones to be investigated in this Note.

2) Instabilities due to **field inhomogeneity fluctuations**. Such instabilities affect *both* echo phase and echo magnitude (in extreme cases, they may completely prevent echo formation).

3) Instabilities due to **fluctuations in spin system parameters** (chemical shifts and scalar couplings). This broad class of phenomena is often lumped under the very broad and generic term chemical exchange (6,7). Though, in principle, such phenomena can also be studied by theoretical methods similar to those adopted here, the topic does not match the scope of this series and shall be pursued in detail elsewhere.

Since most modern NMR instruments employ quadrature phase detection, the echo phase and all its statistical characteristics are experimentally accessible and will be taken into consideration in our analysis.

[1] As usual, the term *'offset'* stands for the difference between Larmor frequency and the phase-detector's 'real' channel RF-reference frequency which provides also the conventional reference for all RF phases.

II. Phase of the n-*th* spin-echo in a CPMG sequence

Let us consider the classical CPMG sequence

$(\pi/2)_x$ - $[\tau$ - $(\pi)_y$ - $\tau]_n$ - acquisition

with various values of n (including n=1 and, as we shall see later, n=0). Clearly, the isolated Hahn echo investigated in Section I is a special case of this sequence for n=1.

Since each $(\pi)_y$ pulse reverses the sign of of the signal phase-accumulation process, the signal phase of the n-th echo at time $2\tau n$ after excitation is given by the integral

$$\phi_n \equiv \phi(2\tau n) = \gamma \int_0^{2\tau n} \chi_n(\tau,t) b(t)\,dt = \gamma \int_{-\infty}^{+\infty} \chi_n(\tau,t) b(t)\,dt\,, \quad [1]$$

where, like in Part I, b(t) is the fluctuating component of the magnetic field, γ the gyromagnetic ratio of the measured nuclei and $\chi_n(\tau,t)$ is the sign-inverting function of time applied in the interval from t=0 to $t=2\tau n$ but, for computational simplicity, zero-extended to the whole range of real values (see Fig.1. for examples). Within the interval $[0,2\tau n]$ the function $\chi_n(\tau,t)$ assumes the values of either +1 or -1, starting with +1 at t=0 and inverting sign synchronously with every $(\pi)_y$ pulse (Fig.1).

By definition, $\langle b(t)\rangle = 0$. Consequently, the mean value of ϕ_n is also null,

$$\langle\phi_n\rangle = 0, \quad [2]$$

while for the variance we obtain (proceeding as in Part I)

$$\langle \phi_n^2 \rangle = \gamma^2 \int_{-\infty}^{+\infty}\int_{-\infty}^{+\infty} \chi_n(\tau,t)\chi_n(\tau,t')\langle b(t)b(t')\rangle\,dt\,dt' \quad [3]$$

$$= (\gamma\sigma)^2(2\tau n)\int_{-\infty}^{+\infty} c(\zeta)\,w_n(\zeta)\,d\zeta$$

where σ is the r.m.s. value of b(t), $c(\zeta)$ is its auto-correlation function normalized to c(0)=1, and

$$w_n(\zeta) = \frac{1}{2\tau n}\int_{-\infty}^{+\infty} \chi_n(\tau,t)\chi_n(\tau,t+\zeta)\,dt\,, \quad [4]$$

The symmetric function $w_n(\zeta)$ is composed of linear segments with their end points located at every multiple of τ (for examples, see Fig.2). It attains its absolute maximum of $w_n(0) = 1$ for $\zeta = 0$ and vanishes for $|\zeta|/\tau \geq 2n$. The values at the points of discontinuity ($|\zeta|/\tau = k$, k=0,1,2,...,2n) fall into 4 series according to the value of m = k mod 4:

$w_n(k\tau) = 1\text{-}k/2n$ when m=0, [5]
$w_n(k\tau) = -1/2n$ when m=1,
$w_n(k\tau) = -1+k/2n$ when m=2 and
$w_n(k\tau) = +1/2n$ when m=3.

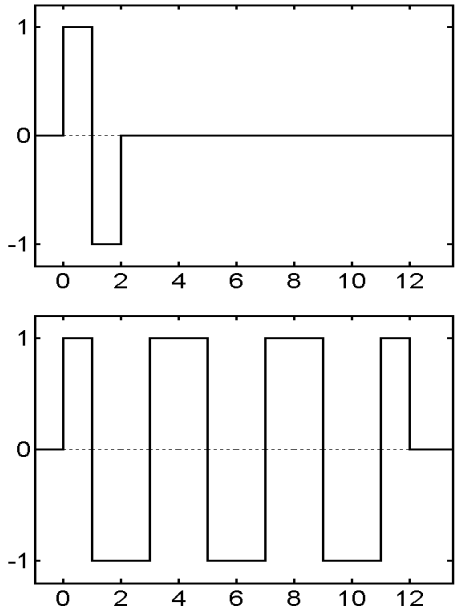

Fig.1. The graphs of $\chi_1(\tau,t)$ (upper) and $\chi_6(\tau,t)$ (lower) against t/τ. The echoes occur at every even value of t/τ.

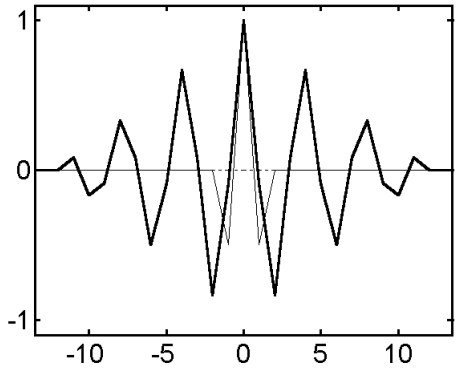

Fig.2.
The functions $w_1(\zeta)$ (thin) and $w_6(\zeta)$ (thick) plotted against ζ/τ.

The function $w_n(\zeta)$ is therefore a *wavelet* (8) and the integral in Eq.[3] can be seen as a *wavelet transform* of the auto-correlation function of field instabilities. It is also evident that for even moderately large n, $w_n(\zeta)$ has a large harmonic content centered around a period of 4τ rather than around 2τ which is a value characteristic of the isolated-echo case $w_1(\zeta)$.

The transition from a period of 2τ (limited to the *fringes* of the χ functions) to one of 4τ (typical for their central portions of the χ functions when n>1) is best understood by comparing the two χ functions shown in Fig.1. This phenomenon is born out by experiment: *in the presence of periodic field modulation with a period T, long CPMG trains are subject to extreme fluctuations in the immediate vicinity of τ = T/4 while single-echo is affected most when τ = T/2*.

Other qualitative features implicit in the shape of $w_n(\zeta)$ regard the limit behavior for very short and very long τ's. It is evident from Eq.[3] that when $c(\zeta)$ drops to zero in a small fraction of τ (field-noise auto-correlation time much shorter than τ), the variance $<\phi_n^2>$ tends to vanish. In the opposite case of τ much shorter then the auto-correlation time, one has to take into account that the mean value of $w_n(\zeta)$ is zero for any n. Consequently, the effects of field fluctuations which are very slow compared to τ also tend to average out (this goes hand-in-hand with the offset re-focussing properties of the CPMG sequence).

III. Explicit formulae for the n-th spin-echo phase variance

When $c(\zeta)$ is an exponential function

$$c(\zeta) = e^{-r|\zeta|/\tau} \qquad [6]$$

with a real or complex parameter r, the integral in Eq.[3] can be computed explicitly. This covers all the most important cases of field fluctuations considered in Part I (stochastic, periodic and quasi periodic). We set

$$s_n(r) = \frac{1}{2\tau}\int_{-\infty}^{+\infty} e^{-r|\zeta|/\tau}\, w_n(\zeta)\, d\zeta = \int_0^{\infty} e^{-rx} w_n(\tau x)\, dx\,, \qquad [7]$$

and cast Eq.[3] into the form

$$<\phi_n^2> = (\gamma\sigma)^2(2\tau n)^2 s_n(r)/n = 2t_n.(\gamma\sigma)^2 T_m\, r s_n(r), \qquad [8]$$

where $t_n = 2\tau n$ is the time between the excitation pulse and the top of the n-th echo.

Let us now evaluate $s_n(r)$. We shall use the following exact formula (9) for exponential integrals of polygonal functions (i.e., functions composed of linear segments):

$$\int_{x_0}^{x_n} e^{-rx} p(x)\, dx = \Delta\left[h(r\Delta)\sum_{k=0}^{n} y_k e^{-rx_k} - \left\{h_0(r\Delta) y_0 e^{-rx_0} + h_n(r\Delta) y_n e^{-rx_n}\right\}\right], \qquad [9]$$

where r is a complex constant, (x_k,y_k), k=0,1,2,...,n, is a sequence of data points with equidistant x-coordinates, p(x) is a function composed of linear segments connecting the consecutive data points, $\Delta = x_{k+1}-x_k$ for every k=0,1,2,...,n-1 and

$$h(\xi) = \{g(-\xi)-g(\xi)\}/\xi = h_0(\xi)+h_n(\xi), \text{ where} \qquad [10]$$

$$h_0(\xi) = \{g(-\xi)-1\}/\xi \text{ and } h_n(\xi) = \{1-g(\xi)\}/\xi = h_0(-\xi), \text{ with } g(\xi) = (1-e^{-\xi})/\xi.$$

Applying Eq.[9] to Eq.[7] we have k=0,1,...,2n, x_k=k, $y_k=w_n(k\tau)$, y_0=1, y_{2n}=0, Δ=1 and ξ = r. Hence

$$s_n(r) = \int_0^{\infty} e^{-rx} w_n(\tau x)\, dx = h(r) S - h_0(r), \quad \text{where} \quad S = \sum_{k=0}^{2n} y_k e^{-kr} \qquad [11]$$

Since the y_k values, given by Eqs.[5] are linear functions of k, the summation can be carried out explicitly using the standard formulae (10)

$$\sum_{k=0}^{n} x^k = \frac{1-x^{n+1}}{1-x} \quad \text{and} \quad \sum_{k=0}^{n} k\, x^k = \frac{x}{1-x}\left\{\frac{1-x^n}{1-x} - n x^n\right\}, \qquad [12]$$

valid for any complex $x \neq 1$ and integer n. Considering Eqs.[5], setting $x = e^{-4r}$, replacing k by $4\kappa+m$ and summing over κ and m separately, one obtains

$$S = S_0 + S_1 + S_2 + S_3 \qquad [13]$$

$$S_0 = \sum_{\kappa=0}^{K_0}\left(1-\frac{2\kappa}{n}\right)x^\kappa = \frac{1}{1-x}\left\{(1-x^{K_0+1})-\frac{2x}{n}\left(\frac{1-x^{K_0}}{1-x}-K_0x^{K_0}\right)\right\}$$

$$S_1 = -\frac{e^{-r}}{2n}\sum_{\kappa=0}^{K_1}x^\kappa = -\frac{e^{-r}}{2n}\frac{1}{1-x}\{1-x^{K_1+1}\}$$

$$S_2 = -e^{-2r}\sum_{\kappa=0}^{K_2}\left(1-\frac{2\kappa+1}{n}\right)x^\kappa = -e^{-2r}\frac{1}{1-x}\left\{\frac{n-1}{n}(1-x^{K_2+1})-\frac{2x}{n}\left(\frac{1-x^{K_2}}{1-x}-K_2x^{K_2}\right)\right\}$$

$$S_3 = \frac{e^{-3r}}{2n}\sum_{\kappa=0}^{K_3}x^\kappa = \frac{e^{-3r}}{2n}\frac{1}{1-x}\{1-x^{K_3+1}\},$$

where[2] $K_0 = n\backslash 2$, $K_1=K_2=(n-1)\backslash 2$, $K_3=(n-2)\backslash 2$ and $S_2=S_3=0$ when $n<2$.

The simplification of these formulae is a cumbersome process which, fortunately, leads to a very compact result[3]. Setting $z=e^{-r}$, one obtains

$$s_n(r) = \frac{h(r)}{1+z^2}\left\{1-\frac{1\pm z^{2n}}{n}\frac{z}{2}\frac{(1-z)^2}{1+z^2}\right\}-h_0(r)\,. \qquad [14]$$

with the upper sign applying to odd n and the lower sign to even n (The fact that odd and even echoes follow slightly different formulae is hardly surprising. Such a difference turns out every time one studies any kind of artifacts related to a spin-echo train). For the first echo, Eq.[14] simplifies to

$$s_1(r) = h(r)(1-z/2)-h_0(r) = \{g(2r)-2g(r)+1\}/r. \qquad [15]$$

IIIa. Random field noise

We shall now discuss the effects of the several special types of field fluctuations (the same which had been considered in Part I). For random field instabilities with r.m.s. value σ and normalized auto-correlation function $c(\zeta) = e^{-|\zeta|/T_m}$ (Part I, Eq.[19]), one can apply Eqs.[8] and [14] *as is* with the real parameter r standing for $r = \tau/T_m$.

It turns out (Fig.3) that in this case the functions $s_n(r)$ exhibit relatively modest variation with respect to the value of n. This feature justifies the form adopted in Eq.[8] which, apart from $s_n(r)$, makes $\langle\phi_n^2\rangle$ proportional to n. It fits with the idea that, for a fixed τ, the phase instabilities of the consecutive echoes in a CPMG train can be treated as a phase-diffusion process and thus lead to an approximate linear dependence of $\langle\phi_n^2\rangle$ on n. In a sense, the residual dependence of the $s_n(r)$ curves on n expresses just the deviations of reality from such a ***phase-diffusion model***.

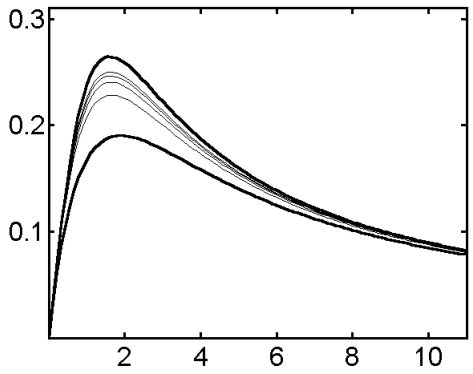

Fig.3. Functions $s_n(r)$ for n=1 (lowermost thick), n=2,3,4,5 (thin) and n=1000 (upper thick).

The derivative of $s_n(r)$ at r=0 is 1/3. Consequently, for $r<<1$ we have $s_n(r) \approx r/3$ -... and, for fixed τ and $T_m\to\infty$,

$$\lim_{T_m\to\infty}\langle\phi_n^2\rangle\, T_m = (\gamma\sigma)^2(2\tau n)^3/6n^2 \qquad [16]$$

indicating that when the field fluctuations become much slower than τ, their effect on the spin-echo phase instability vanishes. Notice the following features valid in the $r<<1$ limit:

- cubic dependence on τ for fixed n
- cubic dependence on the echo time $t=2\tau n$ for fixed n,

[2] When a and b are integers, we denote by $a\backslash b$ the integer part of the ratio a/b.

[3] One must treat separately the first echo, the even echoes and the higher odd echoes (n = 3,5,7,...). It then turns out that the formula for the first echo coincides with the one for higher odd echoes.

- linear dependence on n for fixed τ
- inverse quadratic dependence on n for fixed t.

For large r, s(r) can be approximated by its expansion into powers of r^{-1}.
The first term is $s(r) = r^{-1}$ -... which, for fixed τ, leads to

$$\lim_{T_m \to 0} \langle\phi_n^2\rangle / T_m = 2(\gamma\sigma)^2(2\tau n), \qquad [17]$$

implying that when the field fluctuations are much faster than τ, their effect on spin-echo phase instability also vanishes. In this case, however, we have:

* linear dependence on τ for fixed n
* linear dependence on the echo time $t=2\tau n$ for fixed n,
- linear dependence on n for fixed τ
* no dependence on n for fixed t,

with the asterisks marking a difference compared with respect to the previous case.

For a fixed τ and n, there exists a value of r at which the effect of field fluctuations on the spin echo attains a maximum. Its position is almost independent of n. For n=1 it corresponds $T_m \approx 0.529\tau$ where $r_{max} \approx 1.89$ and $s_1(r_{max}) \approx 0.190$, while for $n \to \infty$ it occurs at $T_m \approx 0.621\tau$, $r_{max} \approx 1.61$ where $s_n(r_{max}) \approx 0.265$. By Eq.[8], the absolute maximum effect of the field noise is therefore given by

$$\langle\phi_n^2\rangle_{max} \approx k_n . n . (\gamma\sigma T_m)^2, \qquad [18]$$

where the constant $k_n = 4 r_{max}^2 s_n(r_{max})$ is nearly independent of n (2.72 for n=1 and 2.75 for $n \to \infty$).

So far, the analysis dealt with a variable T_m which is a point of view of an instrumentation engineer. A more common situation is the one encountered by an end-user who is faced with a given magnet system (fixed T_m) and a possibility to vary τ and n. It is then convenient to write Eq.[8] as

$$\langle\phi_n^2\rangle = 4(\gamma\sigma)^2 T_m^2 \, n \, r^2 s_n(r), \qquad [19]$$

where the τ-dependence, normalized with respect to T_m, is all comprised within the functions $r^2 s_n(r)$ which start with a cubic dependence on τ but then slow down to one which is asymptotically linear. The dependence of the $r^2 s_n(r)$ curves on n is relatively mild.

What does not quite transpire from Fig.3. is the spin-locking capability of the CPMG trains when the echo time $t=2\tau n$ is kept fixed while n is being increased. Let us therefore express $\langle\phi_n^2\rangle$ as a function of the normalized echo-time parameter $t' = (2\tau n)/T_m = t/T_m$. In order to keep t' fixed while varying n, one has to vary τ so that $r \equiv \tau/T_m = t'/2n$. In order to honor the approximate phase-diffusion model, we shall also express explicitly the linear dependence of $\langle\phi_n^2\rangle$ on t', writing

$$\langle\phi_n^2\rangle = (\gamma\sigma)^2 T_m^2 \, t' \, F_n(t'), \qquad [20a]$$

where, according to Eq.[8], the function F_n is given by

$$F_n(t') = 2(t'/2n) s_n(t'/2n), \qquad [20b]$$

This can be compared with an analogous expression for FID phase fluctuations,

$$\langle(\phi_f - \langle\phi_f\rangle)^2\rangle = (\gamma\sigma)^2 T_m^2 \, t' \, F_f(t'), \qquad [20c]$$

where $F_f(t') = 2(1-g(t'))$, which follows from Eq.[20] of Part I.

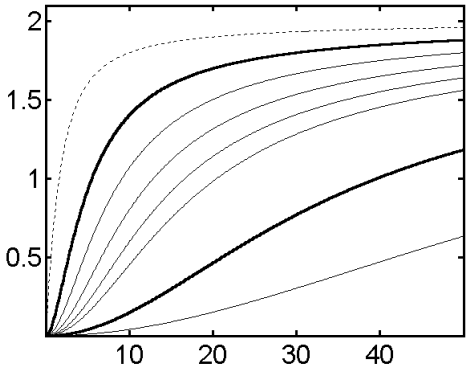

Fig.4.
Functions $F_n(t')$ against the reduced echo-time $t'=t/T_m$, for n=1 (upper thick), 2,3,4,5, 10 (lower thick) and 20 (lowermost). The topmost, dotted curve is $F_f(t')$ pertinent to a simple FID.

The functions $F_f(t')$ and $F_n(t')$ are shown in Fig.4 for several values of n. They illustrate the efficiency with which the insertion of an increasing number n of echoes between the excitation pulse and the signal sampling moment suppresses the leakage of stochastic field fluctuations into the signal phase,

leading in the limit of $n\to\infty$ to a perfect spin-locking even in the presence of quite fast stochastic field fluctuations.

It is also evident that the phase-diffusion model (which would imply a constant value for all the functions) holds only in the limit of $t'\to\infty$ when all the functions become equal to 2. We can really talk about phase diffusion ($F_n(t')$ values above ~1.5) only when $t'>10n$, i.e., $t>10nT_m$.

It is interesting to notice that the function F_f positions itself in the F_n series in a place where we would expect to find the hypothetical function F_0. This interpretation of an FID as the zero-*th* echoes (n=0) seems to be consistent with a number of formulae and situations.

Numeric example for a single echo (n=1): Present FFC magnets are subject to instabilities of the order 25 mGauss rms ($\gamma\sigma$ of about 670 rad/s for protons) with a characteristic time constants of about 0.5 ms. This leads to $<\phi_1^2>=(0.274)^2$ [rad^2] for τ=0.5 ms (probable error of 15.7 degrees) which drops to $<\phi_1^2>=(0.012)^2$ [rad^2] for τ =50 us (probable deviation of 0.68 degree).

IIIb. Periodic field modulation

In order to exploit Eqs.[6-13] in the case of a harmonic auto-correlation function $c(\zeta) = \cos(\omega\zeta)$ (see Part I), one needs to resort to complex-valued arguments r. Considering that $c(\zeta)$ and $w_n(\zeta)$ are both symmetric functions of ζ and $\cos(\omega\zeta)$ is the real part of $e^{j\omega|\zeta|}$, it is evident from Eq.[7] that $s_n(r)$ can be obtained simply by evaluating Eq.[13] with the complex argument $r = -j\omega\tau$ (or $+j\omega\tau$) and taking the real part of the result.

Like in Part I, we shall use the parameter $\rho = \tau/T$, where T is the modulation period. Writing

$$p_n(\rho) = \text{Real}\{s_n(2\pi j\rho)\}/n, \qquad [21]$$

where Real{...} denotes the real part of a complex quantity and $s_n(r)$ is given by Eq.[14], the formula for $<\phi_n^2>$ becomes

$$<\phi_n^2>=(\gamma\sigma)^2(2\tau n)^2 p_n(\rho)\,. \qquad [22]$$

The functions $p_n(\rho)$ can be evaluated numerically for any n using Eqs.[14] and [21]. Several examples are plotted in Fig.5. Comparing these with the results obtained for stochastic fluctuations (Fig.3), one finds both analogies and differences. In particular, keeping τ fixed and varying the period T, we see that the effect of field modulation on the spin echo phase again vanishes for both very short and very long periods.

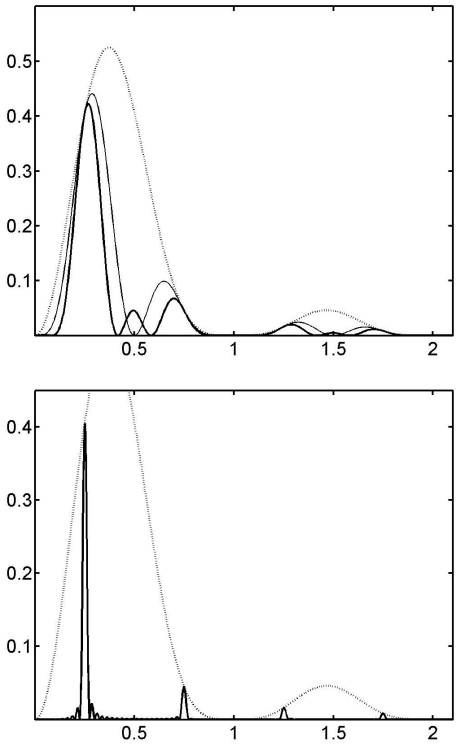

Fig.5. Functions $p_n(\rho)$ for n=1 (dotted), 2 (thin), 3 (thick, upper plot) and 20 (thick, lower plot).

In the important special case of n=1 (single/first echo) one can easily derive the explicit formula

$$p_1(\rho)=\left[\sin^2(\pi\rho)/\pi\rho\right]^2 \qquad [23]$$

which has an absolute maximum at $\rho_{max} \approx 0.37$ with $p(\rho_{max}) \approx 0.525$, accompanied by a series of smaller overtones close to every half-integer ρ.

The new phenomena evidenced by Fig.5 include:

- With increasing n, the location of the absolute maximum shifts rapidly to its limit value of $\rho = 0.25$ (i.e., $\tau = T/4$). This is the T/4 effect anticipated in Section II.

- The main maximum becomes progressively sharper, its half-height width decreasing approximately with 1/n.

- With increasing n, there appear progressively sharper additional maxima (sidebands), located close to every *odd multiple of* T/4.

Fig.5, though useful, does not reflect two common situations often faced by a typical NMR user:

A) Constant echo time $t=2n\tau$ with a variable number n of interposed echoes (τ is then a dependent variable to be adjusted for each n to match the chosen value of t). This is typical of the high-resolution variety of CPMG where the train of echoes is followed by acquisition of delayed FID. The situation also arises in re-focussing sections of complex pulse sequences (n is in these cases usually limited to very low values).

B) The low-resolution CPMG variety where a long train of echoes (often many thousands) is acquired with a fixed τ (usually acquiring just the top of each one). In this case the independent variable is n but the echo time $t=2n\tau$ increases proportionally to n (τ can be viewed as a parameter which defines the proportionality constant).

Case (A): HR-CPMG and re-focussing sequences.

In this case it is best to express $\langle\phi_n^2\rangle$ in terms of the normalized-time parameter $t'= t/T$ as

$$\langle\phi_n^2\rangle = (\gamma\sigma T)^2 P_n(t'), \qquad [24]$$

where the functions $P_n(t') = t'^2 p_n(t'/2n)$ are expected to be periodic. In particular, we expect the maxima to coincide with $\tau=(2k+1)(T/4)$ and therefore $t'=n(k+1/2)$, where k=0,1,2,... The plots in Fig.6 show that this is indeed the case - plus a number of additional and not quite intuitive features which become evident when $n\geq 3$:

- The maxima are surprisingly high, exceeding substantially those encountered in an FID (Part I, Fig.4, $\kappa=0$). It follows that, *at selected values of τ, the CPMG echo train selectively amplifies the field modulations rather than re-focussing them*. The amplification at $t'/n=k+1/2$ thus has all the features of a *resonance phenomenon*. Consider that the effect of the same periodic disturbance on the phase of a simple FID is described by the function, easily deduced from Eq.[29] of Part I,

$$P_f(t') = (1/\pi^2)\sin^2(\pi t'/n) \qquad [25]$$

which is periodic with a maximum value of just about 0.10. In comparison, even $P_1(t')$ has maxima which are 4 times higher (about 0.405) and the peak values of $P_n(t')$ tend to grow linearly with n.

- At t' values which surround odd multiples of n (we shall refer to these as the *odd intervals*), there is a comb-like pattern of fringe peaks (n-2 in total) which are small with respect to the main maxima but still substantially larger than the $P_f(t')$ maxima (the values of smallest ones in the central part seem to be consistently about 0.4 - the same height as the $P_1(t')$ lobes). In the local valleys between these fringe peaks, there are n-2 equidistant points where re-focussing is perfect. It is therefore rather difficult to say anything definite about the odd intervals without a careful prior analysis of the *exact* value of t'/n.

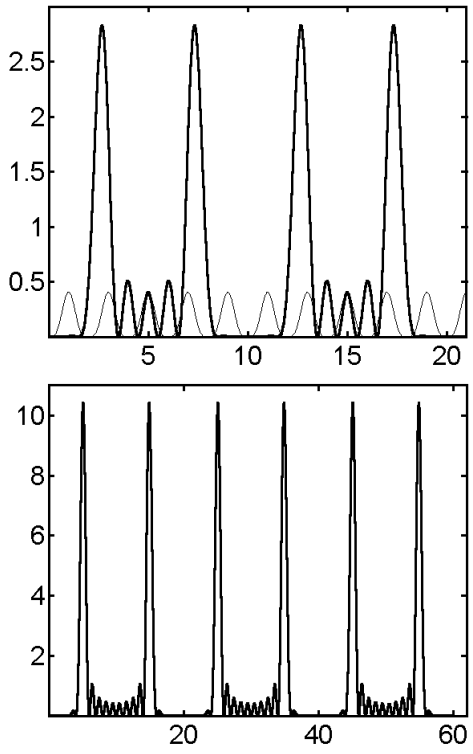

Fig 6.
Examples of the functions $P_n(t')$ for n=1 (upper graph, thin), n=5 (upper graph, thick) and n=10 (lower graph)

- There is an excellent re-focussing at t' values which surround even multiples of n (the *even intervals*). The even intervals fringe peaks, though present in the same number as their odd counterparts, are much smaller and virtually vanish around the center of the intervals, with the excellent re-focussing region covering over half of each even interval.

Case (B): LR-CPMG.

To handle this case, it is convenient to rewrite Eq.[22] as

$$<\phi_n^2> = (\gamma\sigma T)^2 P_\rho(n), \quad \text{where} \quad P_\rho(n) \equiv (2\rho)^2 n^2 p_n(\rho) \ . \qquad [26]$$

The function $P_\rho(n)$ defines completely the dependence of $<\phi_n^2>$ on n. The rather spectacular behavior of $P_\rho(n)$ is exemplified for various values of ρ in Fig.7.

The upper graph in Fig.7 shows the propagation of the field modulation into the first 120 echoes for values of $\rho \equiv \tau/T$ comprised between 0 and 0.25. Its variation over 5 decades shows how the excellent field re-focussing at low ρ values progressively turns over into a resonant amplification when ρ approaches the critical value of 0.25. This, however, does not necessarily happen uniformly for all the echoes.

Consider, for example, the curve $P_\rho(n)$ for ρ = 0.23 (upper graph, bold). First of all, it is periodic with a period[4] of

$$n_p = \text{abs}(1/[2(\rho-0.25)]), \qquad [27]$$

which for ρ = 0.23 gives n_p = 25. Consequently, every 25-th echo is not influenced by the field fluctuations at all, while the in-between echoes are influenced very strongly (roughly 50 times more than an FID).

In the limit of ρ = 0.25, the periodicity disappears (infinite cycle length) and there is a linear accumulation of the perturbation throughout the echo train. The phenomenon is so pronounced that even a *slight inhomogeneity of the periodic field perturbation across the sample* (a possibility which we have not included in our assumptions) eventually compromises the echo formation. Experimental data (to be discussed later) bore out all the implications of Eq.[26] everywhere except in a very close vicinity of the critical ρ values where not just phases but also the magnitudes of the echoes may be strongly affected at large values of n.

Compared with an FID, the break-even point occurs at ρ ≈ 0.168 (upper graph, lowermost curve) in the sense that below that value no echo is influenced more than any point in an FID at the same time since excitation.

The bottom graphs in Fig.7 provide a comparison between the functions $P_\rho(n)$ for a few values of ρ distributed in a similar manner within the *odd interval* 0.25 ≤ ρ ≤ 0.75 and within the even interval 0.75 ≤ ρ ≤ 1.25. The following features become evident:

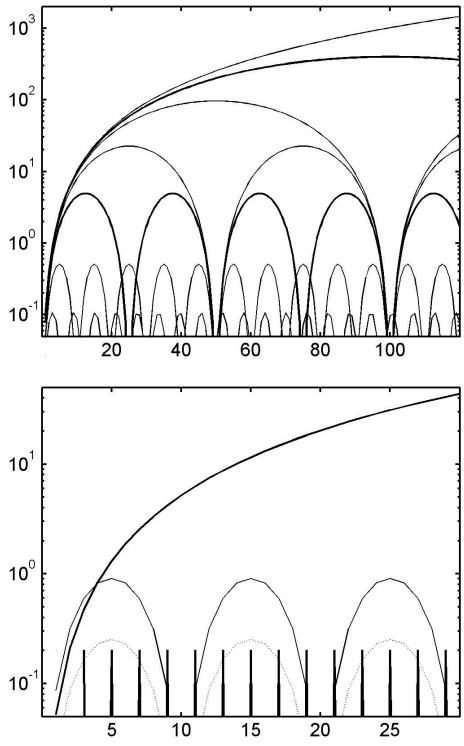

Fig. 7.
Semilog plots of the functions $P_\rho(n)$ for various values of the parameter ρ.
- *Top* (ρ≤0.25), listed in the order of decreasing maximal values: ρ = 0.25, 0.2475 (bold), 0.245, 0.24, 0.23 (bold), 0.2 and 0.168.
- *Bottom*: ρ = 0.2525 and 0.7475 (bold), 0.3 and 0.7 (thin), 0.5 (comblike), 0.8 and 1.2 (dotted) and 1.0 (not visible; lies below the graph edge).

- At a comparable distance of ρ from the nearest critical value, the disturbances are more pronounced within the odd intervals 0.5k -0.25 ≤ ρ ≤ 0.5k+0.25 than in the even ones.

- Within each interval, the two functions $P_{0.5k-\rho}(n)$ and $P_{0.5k+\rho}(n)$ are identical (reflection symmetry with respect to the center of the interval.

- Naturally, since $P_\rho(n)$ is periodic with respect to ρ with a period of 1, all the even intervals are identical and so are all the odd intervals.

[4] Analytical inspection of the function $p_n(\rho)$ and all the functions derived from it is not at all easy but some of its features, such as the n-period mentioned here, can be deduced relatively easily. The explicit math, however, does not add much to the insights gained by the numeric approach and is therefore skipped.

IIIc. Quasi-periodic field modulation

The most generic case to which Eqs.[6-13] can be applied is characterized by the auto-correlation function $c(\zeta) = e^{-|\zeta|\kappa\omega}\cos(\omega\zeta)$, describing quasi-periodic field fluctuations (see also Part I) with a center frequency ω and a frequency spread of $2\kappa\omega$ (k being a dimensionless factor). Again, considering that $c(\zeta)$ and $w_n(\zeta)$ are both symmetric functions of ζ and $e^{-|\zeta|\kappa\omega}\cos(\omega\zeta)$ is the real part of $e^{(i-\kappa)\omega|\zeta|}$, it is evident from Eq.[7] that $s_n(r)$ can be obtained simply by evaluating Eq.[13] with one of the the complex arguments $r = (\kappa \pm j)\omega\tau$ and taking the real part of the result. We shall again use the parameter $\rho = \tau/T$, where $T=2\pi/\omega$ is the central period. Writing

$$p_n(\rho,\kappa) = \text{real}\{s_n[2\pi\rho(\kappa \pm j)]\} / n, \qquad [28]$$

where $s_n(r)$ is given by Eq.[14], the formula for $\langle\phi_n^2\rangle$ becomes

$$\langle \phi_n^2 \rangle = (\gamma\sigma)^2 (2\tau n)^2 p_n(\rho,\kappa)\,. \qquad [29]$$

For $\kappa=0$, the functions $p_n(\rho,\kappa)$ coincide with the $p_n(\rho)$ of the previous case so that we can expect the present case to be a generalization of the previous one. It is not immediately obvious, however, what is the impact of the modulation frequency instability on the resonance effects discussed above.

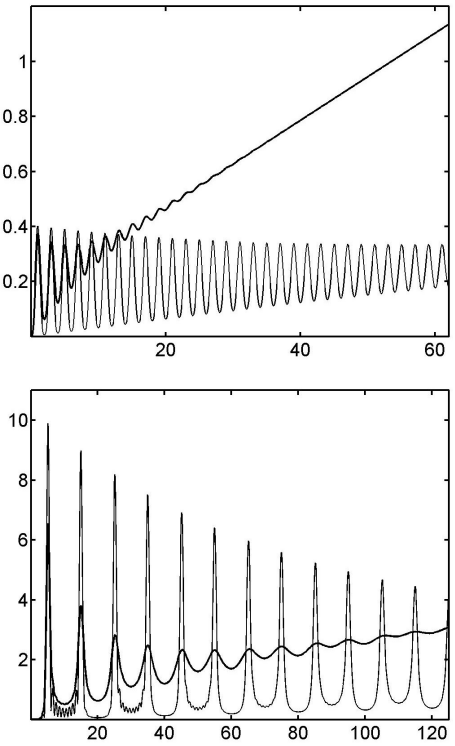

Fig 8.
$P_{n,\kappa}(t')$ plotted for various values of n,κ:
n = 1 (top graph) and 10 (bottom graph)
κ = 0.005 (thin) and 0.05 (bold)

Using Eqs.[28] and [29], we can inspect the effect of non-zero κ on the two special cases (i.e., on Figures 6 and 7).

Case (A): HR-CPMG and re-focussing

Rewriting Eq.[24] as

$$\langle\phi_n^2\rangle = (\gamma\sigma T)^2 P_n(t',\kappa), \qquad [30]$$

where $P_{n,\kappa}(t')=t'^2 p_n(t'/2n,\kappa)$, Fig.6 gets modified as shown in Fig.8 for a two values of n and for κ = 0.005 and 0.05 (1% and 10% instability in the modulation frequency, respectively). These are to be compared with the n=1 and n=10 cases of Fig.6 where κ = 0.

The result is a progressive damping of the oscillatory, resonance pattern and the appearance of a growing phase-diffusion component. This is similar to the results obtained for plain FID in Part I.

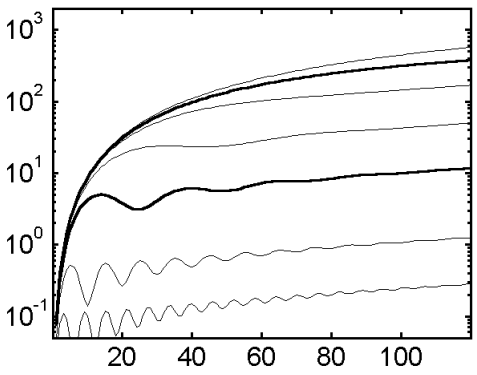

Fig.9
$P_{\rho,\kappa}(n)$ plotted for κ=0.005 and the following ρ-values (top down): 0.25, 0.2475 (bold), 0.245, 0.24, 0.23 (bold), 0.2 and 0.168.

We shall postpone further discussion of these effects but one more feature should be pointed-out right now. For higher values of n (as evidenced for n=10 in the lower graph of Fig.8) the initially marked distinction between the even and odd intervals tends to get 'filtered out' by even modest fluctuations in the modulation frequency. What disappears still faster is the fine pattern of fringe peaks between the principle resonance peaks. It is also interesting that there are regions where the peak values of $P_{n,\kappa}(t')$ decrease with increasing κ.

Case (B): LR-CPMG

The generalized Eq.[26] is

$$< \phi_n^2 >= (\gamma\sigma T)^2 P_{\rho,\kappa}(n) \ , \qquad [31]$$

$$P_{\rho,\kappa}(n) \equiv (2\rho)^2 n^2 p_n(\rho,\kappa) \ .$$

The functions $P_{\rho,\kappa}(n)$ are shown in Fig.9 for κ=0.01 (corresponding to just 2% instability in the modulation frequency). This is to be compared with the upper graph of Fig.7 corresponding to κ=0. The result is again a surprisingly efficient damping of the oscillatory pattern combined with a modest phase-diffusion contribution. Most important is the fact that i) no echoes are now exempt from the perturbation and ii) with increasing κ, $P_{\rho,\kappa}(n)$ tends to a value which is only moderately lower than the maxima of $P_\rho(n)$, indicating that the resonance effect is to a large extent still present.

IV. Propagation of field-noise errors into accumulated spin-echo data

We shall now concern ourselves with the effects of field noise on the amplitudes of accumulated data whose generation involved one or more spin-echoes. To evaluate these second-order effects (in the first order the phase errors average to zero) we shall apply the theoretical principles introduced in Part I. It should be pointed out, however, that first-order phase error effects may have a more severe impact when re-focussing spin-echo pulse-sequence sections are used as building blocks of more complex pulse sequences which in some cases rely on their phase stability.

When data are accumulated in a standard way through repeated scans, there remains a second-order bias. Following step-by-step the arguments which led to Eqs.[10] and [11] of Part I (the only difference consisting in the replacement of $\phi_f(t)$ by ϕ_n), it is easily shown that:

i) The effect on the accumulated echo amplitude is expressed by the multiplicative factor

$$G_n = <\exp[j\phi_n]>. \qquad [32]$$

ii) In the case of a normally distributed, Gaussian field noise, Eq.[32] evaluates to

$$G_n = \exp(-<\phi_n^2>/2). \qquad [33]$$

Non-Gaussian and/or mixed cases like the ones of periodic and quasi-periodic perturbation shall be also treated following the methods outlined in Part I (Eqs.[32] and [38] therein).

IVa. Random field-noise

Since Eq.[33] is in this case exactly applicable, we can combine it with Eq.[8], obtaining

$$G_n = \exp(-<\phi_n^2>/2) = \exp[-(\gamma\sigma)^2(2\tau n)^2 s_n(r)/2n]$$
$$= \exp[-(2\tau n)\,(\gamma\sigma)^2 T_m\, r s_n(r)], \qquad [34]$$

where $s_n(r)$ is given by Eq.[14] and, as usual, $r=\tau/T_m$.

Eq.[34] has many practical consequences, the most notable of which are the errors it introduces into the measurements of the relaxation times T_2. Regardless of whether a HR-CPMG or a LR-CPMG sequence is used for this purpose, one always sets up a fixed τ and measures the decay of the echo with respect to increasing echo number n which is proportional to the elapsed echo time $2\tau n$. The decay is affected by T_2, homonuclear spin-spin couplings (the J's), 'chemical exchange', spin diffusion, and convective flow (the latter two in the presence of

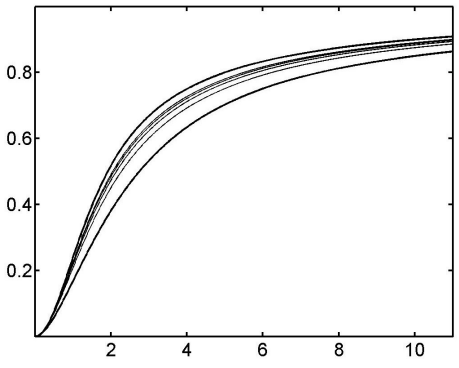

Fig.10.
The functions $rs_n(r)$ for n=1 (lowest curve), n=2,3,4,5 (the thin curves) and n=1000 (the upper curve).

sufficiently strong field gradients). In the limit of $\tau \to 0$ only the T_2 process remains effective[5] and the n-th echo signal is given by $S(t_n) = S_0 \exp(-2\tau n R_2) = S_0 \exp(-t_n R_2)$, where $R_2 = 1/T_2$ is the relaxation rate. In the presence of random field noise, S_n must be multiplied by G_n so that, for averaged CPMG decays,

$$S(t_n) = S_0 \exp\{-t_n [R_2 + w\, rs_n(r)]\}, \qquad [35]$$

where $w = (\gamma\sigma)^2 T_m$.

The effect can be described as an extra contribution of $wrs_n(r)$ to the apparent relaxation rate T_2. The factor $rs_n(r)$, plotted in Fig.10, has only a modest dependence on n which is limited to a few starting echoes. The distortion of S_n is essentially mono-exponential except for the fact that the starting echoes (n = 1 to 5) are a bit *lower* than expected. Since $rs_n(r)$ tends towards 1 for large values of $r = \tau/T_m$, the extra contribution to R_2 tends towards w, while it vanishes for small tau values. Using a suitable substance (one void of any inherent τ-dependence of the CPMG decay), the dependence of the extra contribution on τ can be used to empirically assess the quantities $(\gamma\sigma)$ and T_m.

IVb. Periodic field modulation

By Eq.[32] of Part I, the effect of the field modulation on the accumulated n-th echo signal is its multiplication by the real factor $G_{c,n}$ (the index c stands for 'cyclic')

$$G_{c,n} = J_0\left(\sqrt{2 < \phi_n^2 >}\right) = J_0\left(2\sqrt{t_n w_c R_\rho(n)}\right), \qquad [36]$$

where $w_c = (\gamma\sigma)^2 T$, $R_\rho(n) = \rho\, \mathrm{Real}\{s_n(2\pi j\rho)\}$, and the last expression has been obtained using Eqs.[21] and [22].

Fig.11 illustrates the function $R_\rho(n)$ for a few values of ρ in the vicinity of the resonant critical value of $\rho = 0.25$. It shows that significant distortions occur only when ρ is quite close to the critical value and, unless it is too close, they affect only a relatively limited number of starting echoes. It should be kept in mind, however, that what we are discussing here are the second-order effects on the CPMG decays averaged over a potentially infinite number of scans. Even when such effects appear small, the first-order phase instabilities, appearing as a severe decay irreproducibility, force the instrument operator to dramatically increase the number of scans to be taken.

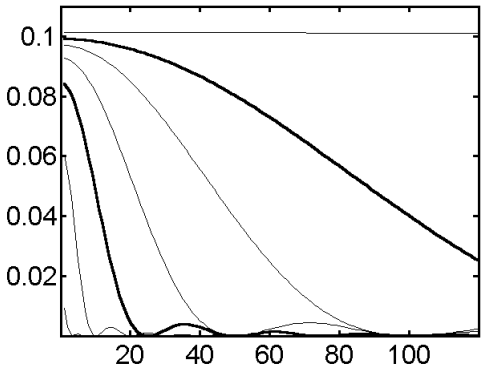

Fig.11.
Functions $R_\rho(n)$ for the following values of the parameter $\rho = \tau/T$ (top to bottom): 0.25, 0.2475 (thick), 0.245, 0.24, 0.23 (thick), 0.2 and 0.1

In most practical cases, the Bessel function in Eq.[32] can be approximated by a Gaussian, exploiting the fact that, for $|x|<1$, $\exp(-x^2/4) \approx J_0(x)$ with an error smaller than 0.014. When $2w_c R_\rho(n) < 1$ we therefore have $G_{c,n} \approx \exp\{-t_n w_c R_\rho(n)\}$ so that

$$S(t_n) = S_0 \exp\{-t_n R_2\}\, G_{c,n} \qquad [37a]$$

$$\approx S_0 \exp\{-t_n [R_2 + w_c R_\rho(n)]\}, \qquad [37b]$$

where Eq.[37a] is the exact formula and Eq.[37b] is the approximation.

In the case of transverse-relaxation measurements, the quantity $w_c R_\rho(n)$ can be viewed as the field-modulation bias imposed upon R_2 should the latter be determined simply from the attenuation of the n-th echo at time t_n.

The upper graph in Fig.12 illustrates the effect of periodic field modulation on averaged experimental CPMG decays. Notice that the example implies $(\gamma\sigma)^2 = 1000\ \mathrm{rad}^2$ so that $\gamma\sigma \approx 32$ rad, a value corresponding

[5] In some cases this is an oversimplification but that does not really have any impact on our discussion.

for protons to a mains-related field-modulation amplitude of about 0.12 μT which, for a normal laboratory environment, is a relatively small value.

IVc.Quasi-periodic field modulation

As discussed in Section IIIc, in the case of unstable modulation frequency with an instability factor κ one needs to replace the $R_\rho(n)$ of Eq.[36] with $R_\rho(n) = \rho\ \text{real}\{s_n[2\pi\rho(\kappa \pm j)]\}$. Moreover, one should separate the transient oscillatory component of $<\phi_n^2>$ from the linear phase-diffusion term and then use the former in a Bessel weighing factor and the latter in a Gaussian one (see what has been done for the FID's in Section IIIc of Part I). Unfortunately, unlike in the case of FID's, it appears very difficult to carry out the separation (except, perhaps, by numerical means).

Figures 8 and 9 indicate, however, that even very small modulation frequency instabilities lead to an efficient damping of the oscillations which means that the Gaussian weighing factor should in most cases prevail. Since, as we have seen in the preceding Section, the Gaussian approximation is reasonable even for κ=0, it can be expected to be quite good for any κ (except perhaps when κ is extremely small and ρ is extremely close to one of the critical values).

The lower graph in Fig.12 exemplifies the effect of a non-zero value of κ evaluated using both the Gaussian approximation of Eq.[37b] and the 'Bessel approximation' of Eq.[37a]. On the basis of the preceding discussion (and of Fig.9) we expect the 'exact' curves to stay always between these extreme cases and to fall closer to the Gaussian one for any κ greater than about 0.005.

As expected, the effect of non-zero κ is to mitigate the resonance-like effects for ρ lying in the vicinity of the critical value. Moreover, notice that some of the distorted curves could be easily mistaken for bi-exponential decays.

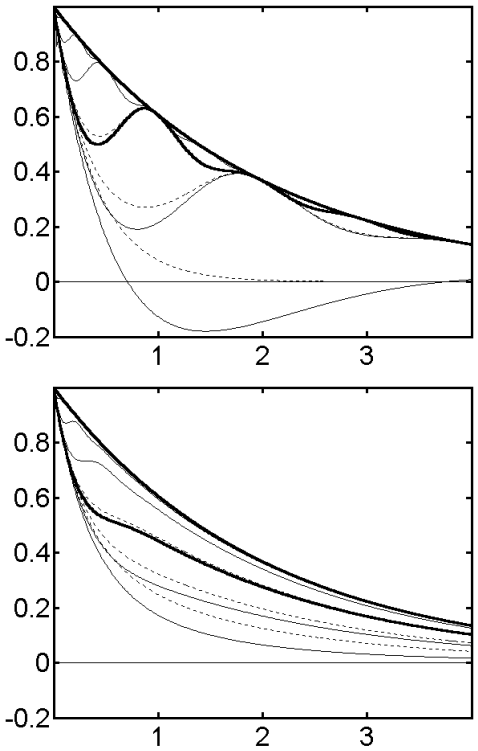

Fig.12.

Upper graph: Plot of an averaged CPMG decay $S(t_n)$ for T=20 ms, R_2=0.5 s^{-1}, $w_c \equiv (\gamma\sigma)^2 T$= 20 $rad^2 s^{-1}$, and, form bottom up, ρ = 0.25, 0.2475, 0.245 (thick), 0.24, 0.23, 0.2 and 0.1 (overlapping the true decay). The dotted traces are Gaussian approximations (Eq.[37b]) to the nearest exact curves (coincidend for $\rho \leq 0.24$).

Lower graph: As above but with modulation frequency instability factor of κ =0.01. The Gaussian approximations are in this case expected to be closer to reality (see text).

V. Conclusions

We have shown how the phase noise due to magnetic field instabilities propagates into isolated, as well as multiple NMR echoes. Identical effects might be due also to the phase noise of the receiver reference frequency (this, however, is normally expected to be far too small to cause any problems).

After delimiting three basic typical types of magnetic field noise (random, periodic, and mixed), we have derived specific formulae covering the individual cases. The mathematics which emerges is rather complex but, at the same time, quite fascinating.

It turns out that long trains of periodically repeated pulses like those used in the CPMG sequence interact with the corresponding frequency components of magnetic field fluctuations in a highly selective way. This has many obvious consequences in terms of understanding instrumental artifacts and proper planning of experiment involving single- and, in particular, multiple- echoes.

So far we have discussed only the artifacts due to the statistical bias of signal phase projections which can be appreciated in averaged echoes and echo trains. One should also try and establish some of the statistical characteristics of single-scan echoes and echo trains and, more generally, those characteristics which pertain to the averages obtained after a limited number of scans. The route towards such statistics has been paved but the ground which it opens is yet to be explored.

Some practical consequences of this study have been already pointed out (mostly in Section IV). Of particular practical value are the predictions (both qualitative and quantitative) regarding the field-noise contribution to the apparent value of the measured T_2's and the emergence of an anomalous non-exponential behavior of CPMG-decays. Clearly, however, there is still much more to be done.

References:

1. Sykora S., *Field noise effects on NMR signals: FID's and 1D Spectra*,
   Stan's Library, Vol.I., March 2006 (*www.ebyte.it/library/Library.html*).
   Available at *http://www.ebyte.it/library/docs/nmr06a/NMR_FieldNoise_Fid.html*.
   See also the poster on *Field-Noise Effects in NMR*,
   presented at *XXXIV Congress on Magnetic Resonance*, GIDRM, Porto Conte, Italy 2004,
   available at *http://www.ebyte.it/stan/Poster_NmrFieldNoise.html*.
2. Hahn E.L., *Spin echoes*, Phys.Rev. **80**, 580-594 (1950).
3. Carr H.Y., Purcell E.M., *Effects of diffusion on free precession in nuclear magnetic resonance experiments*,
   Phys.Rev. **94**, 630-638 (1954).
4. Meiboom S., Gill D., *Modified spin-echo method for measuring nuclear relaxation times*,
   Rev.Sci.Instruments **29**, 688 (1958).
5. Allerhand A., *Effect of Magnetic Field Fluctuations in Spin-Echo NMR Experiments*,
   Rev.Sci.Instruments **41**, 269 (1970).
6. Gutowsky H.S, Vold R.L, Wells E.J., *Theory of Chemical Exchange Effects in Magnetic Resonance*,
   J.Chem.Phys. **43**,4107 (1965).
7. Allerhand A, Gutowsky H.S, Jonas J, Meinzer R.A.,
   NMR Methods for Determining Chemical-Echange Rates, J.Am.Chem.Soc. **88**,3185 (1966).
8. Walnut D.F., *An Introduction to Wavelet Analysis*, Birkhauser 2004.
9. Sykora S., Exponential Transforms of Polygonal Functions,
   Stan's Library, Vol.I., May 2006 (*www.ebyte.it/library/Library.html*).
10. Sykora S., *Finite and Infinite Sums of the Power Series (k^p)(x^k)*,
    Stan's Library, Vol.I., April 2006 (*www.ebyte.it/library/Library.html*).

This study was carried out during the years 2003-2005